
Comparison of particle-tracking and lumped-parameter age-distribution models for evaluating vulnerability of production wells to contamination

S. M. Eberts · J. K. Böhlke · L. J. Kauffman ·
B. C. Jurgens

Abstract Environmental age tracers have been used in various ways to help assess vulnerability of drinking-water production wells to contamination. The most appropriate approach will depend on the information that is available and that which is desired. To understand how the well will respond to changing nonpoint-source contaminant inputs at the water table, some representation of the distribution of groundwater ages in the well is needed. Such information for production wells is sparse and difficult to obtain, especially in areas lacking detailed field studies. In this study, age distributions derived from detailed groundwater-flow models with advective particle tracking were compared with those generated from lumped-parameter models to examine conditions in which estimates from simpler, less resource-intensive lumped-parameter models could be used in place of estimates from particle-tracking models. In each of four contrasting hydrogeologic settings in the USA, particle-tracking and lumped-parameter models yielded roughly similar age distributions and largely indistinguishable contaminant

trends when based on similar conceptual models and calibrated to similar tracer data. Although model calibrations and predictions were variably affected by tracer limitations and conceptual ambiguities, results illustrated the importance of full age distributions, rather than apparent tracer ages or model mean ages, for trend analysis and forecasting.

Keywords Groundwater age · Contamination · Numerical modeling · Water supply · USA

Introduction

Drinking-water production wells commonly produce water with a wide range of groundwater ages (range of travel times from the water table to the well). The responses of such wells to transient distributed watershed contamination can be highly variable, as different fractions of the produced water will contain varying amounts of contaminants, depending on their ages and source areas. A number of states and local communities in the United States have used information on groundwater age to assess the vulnerability of their groundwater sources of drinking water. For example, tritium has been used to identify aquifers and production wells that contain some young water (< 60 years) that may be vulnerable to contamination from near-surface sources (e.g., Michigan DEQ 2009).

The most appropriate application of environmental tracer data to problems of well vulnerability will depend upon the specific information that is desired. For example, if the intent of a vulnerability assessment is to recognize whether a well may be impacted by nonatmospheric sources of anthropogenic contaminants, it may be sufficient to measure low-level concentrations of many potential contaminants in discharge from the well. Plummer et al. (2008) describe a classification for assessing vulnerability at the scale of individual wells based on the number of halogenated volatile organic compound (VOC) detections along with the total dissolved VOC concentrations in samples from the wells. If what is desired is an estimate of the fraction of the water

Received: 18 February 2011 / Accepted: 14 November 2011

© Springer-Verlag (outside the USA) 2011

Electronic supplementary material The online version of this article (doi:10.1007/s10040-011-0810-6) contains supplementary material, which is available to authorized users.

S. M. Eberts (✉)
US Geological Survey,
6480 Doubletree Ave., Columbus, OH 43229, USA
e-mail: smeberths@usgs.gov
Tel.: +1-614-4307740
Fax: +1-614-4307777

J. K. Böhlke
US Geological Survey,
431 National Center, Reston, VA 20192, USA

L. J. Kauffman
US Geological Survey,
810 Bear Tavern Rd., Ste. 206, West Trenton, NJ 08628, USA

B. C. Jurgens
US Geological Survey,
Placer Hall – 6000 J St., Sacramento, CA 95819, USA

that is young enough to have recharged within the last 60 years, samples can be analyzed for an ensemble of environmental tracers that have had different atmospheric input histories (Nelms et al. 2003; Manning et al. 2005). If information on the probability of occurrence of young, unmixed groundwater (e.g., water with a discrete age less than 60 years) is of interest, a logistic regression model based on atmospheric environmental tracers can be developed (Rupert and Plummer 2009). If the objective of a vulnerability assessment is to understand how a well will respond to changing nonpoint-source contaminant inputs at the water table, knowledge of the full distribution of groundwater ages in the water produced by the well is important.

The groundwater-age distribution at a production well is a function of (1) the age distribution of water in the aquifer and (2) the interaction of the well with the aquifer (Maloszewski and Zuber 1982; Einarson and Mackay 2001; Böhlke 2002; Frind et al. 2006; Katz et al. 2007; Zinn and Konikow 2007; Jurgens et al. 2008; Landon et al. 2008). Because the placement, construction, and operation of a well dictate the portion of the groundwater-age distribution in an aquifer that is sampled by the well, even wells within a single aquifer system can produce water with different age distributions, and therefore may respond differently to human activities near the land surface.

The spatial distribution of groundwater ages in aquifers, and the frequency distribution (or fractional abundance) of ages in discharge from wells and springs, have been studied extensively through the use of environmental tracer analysis and modeling (e.g., Maloszewski and Zuber 1982; Bethke and Johnson 2008). Models with differing levels of complexity have been used to characterize age distributions of water at production wells and to simulate the responses of such wells to contamination. In a general sense, this may involve (1) inverse modeling of physical data and environmental tracer data from groundwater samples to derive hydraulic parameters and flow fields, followed by (2) forward modeling of transient contaminant inputs using the previously established physical models. The distinction between environmental tracers (phase 1) and contaminants (phase 2) may be somewhat arbitrary, as they may be treated similarly in the models and may be interchangeable in some cases. Three-dimensional distributed-parameter groundwater-flow models with particle tracking have been used by numerous investigators to help anticipate the effects on production wells of nonpoint-source contaminant loading at the water table (e.g., Kauffman et al. 2001; Zoellmann et al. 2001; McMahon et al. 2008a, b). An approach based on adjoint theory that combines forward- and backward-in-time transport modeling was used by Frind et al. (2006) to simulate the expected impact at a wellfield of potential contaminant sources at unknown locations within the capture zone. Groundwater-age distributions from lumped-parameter models also have been coupled with contaminant input functions to explore contaminant responses at production wells (e.g., Böhlke 2002;

Osenbrück et al. 2006). This approach builds upon well-established precedents for evaluating age distributions and mean ages of discharge using lumped-parameter models (for example, linear, exponential, or dispersion models) and environmental tracer data (e.g., Maloszewski and Zuber 1982, 1993; Amin and Campana 1996; Cook and Böhlke 2000; Ozyurt and Bayari 2005). The lumped-parameter modeling approach has its roots in chemical engineering (Levenspiel 1999); early application to the field of hydrology is described in Nir (1986).

Despite many and varied applications of environmental tracer analysis and modeling to characterize groundwater ages in aquifers and watersheds, direct comparisons of age distribution results from distributed- and lumped-parameter models for drinking-water production wells or natural groundwater discharge are relatively limited (e.g., Scanlon et al. 2003). The purpose of this paper is to compare (1) the ability of the different models to match observed tracer concentrations in a typical production well in each of several contrasting hydrogeologic settings, and (2) predicted responses at the wells to a change in nonpoint-source contaminant input based on the simulated age distributions. The field sites are located within four aquifer systems, which together supplied 35% of the water used for public supply in the United States in 2000 (Maupin and Barber 2005): Modesto, California (Central Valley aquifer system); Tampa, Florida (Floridan aquifer system); Woodbury, Connecticut (Glacial aquifer system); and York, Nebraska (High Plains aquifer) (Fig. 1 and Table 1; Eberts et al. 2005). The model approaches are: distributed-parameter groundwater-flow models with advective particle tracking (Harbaugh et al. 2000; Pollock 1994) and lumped-parameter models, including the linear model (L), the exponential model (E), the exponential piston-flow model (EP), and the dispersion model (DM) of Maloszewski and Zuber (1982, 1993). In addition, two binary mixing models (BEP, BPP) involving younger and older components with differing age distributions were applied (Table 1). All models were calibrated using inverse methods to multiple environmental-tracer measurements. The distributed-parameter flow models summarized herein have been described previously (Burow et al. 2008; Crandall et al. 2009; Starn and Brown 2007; Clark et al. 2007), whereas the lumped-parameter models and comparisons are new. Discussions focus on the utility of the different approaches for informing source-water protection decisions and assessing production-well vulnerability to nonpoint-source contamination. The different field sites illustrate differences in the complexity of the approaches and sensitivity of the results in some important types of aquifer settings.

Hydrogeologic settings

The *Modesto, California* study area has a semiarid climate and receives an average of 315 mm of precipitation per year. Irrigation in the agricultural area just outside of Modesto has increased groundwater recharge rates to

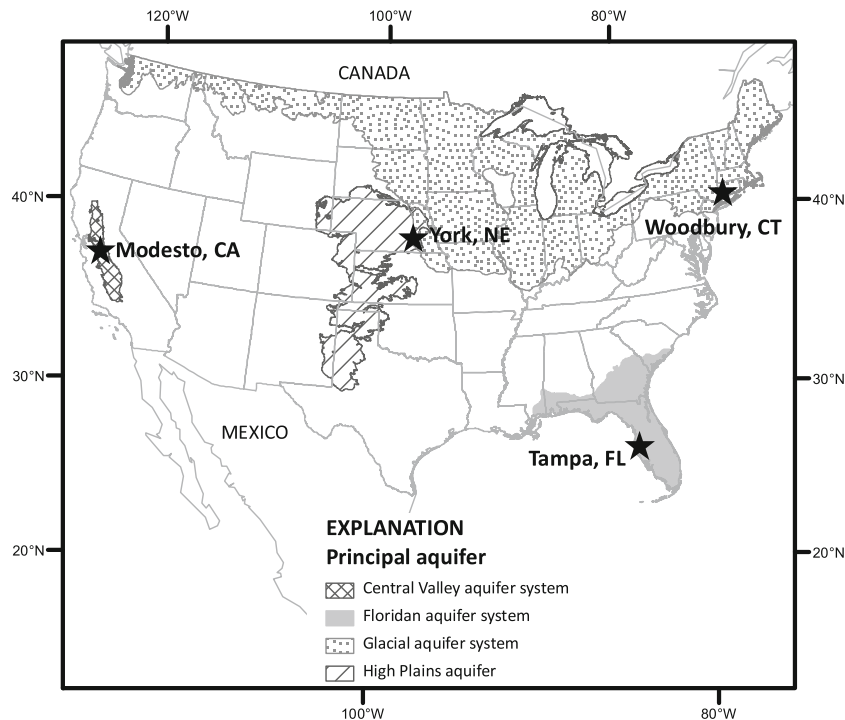


Fig. 1 Location of the principal aquifers and communities in the USA where production wells were studied (see Table 1)

more than 600 mm/year in some locations. The selected production well is located in the urban area and is screened in a series of unconsolidated alluvial-fan sediments comprised of lenses of gravel, sand, silt, and clay (Table 1 and Fig. 2a). The aquifer is unconfined in the shallow part of the system, becoming semiconfined with depth. Depth to water was about 10 m (Jurgens et al. 2008; Burow et al. 2008).

The Tampa, Florida study area has a subtropical, humid climate and receives an average of 1,140 mm of precipitation per year. The selected production well is open to a sequence of carbonate rocks with karst

features (Table 1 and Fig. 2b). The upper part of the Floridan aquifer from which the well produces is overlain by a discontinuous confining unit composed of dense plastic green-gray clay, interbedded with varying amounts of chert, sand, clay, marl, shell, and phosphate. This intermediate confining unit is locally breached by sinkholes associated with the underlying carbonate rock. Overlying the intermediate confining unit are unconsolidated sands, clays, and marls that constitute an unconfined surficial aquifer system. Depth to water was within 3 m of land surface (Katz et al. 2007; Crandall et al. 2009).

Table 1 Characteristics of selected production wells, lumped-parameter models and tracers used to help calibrate the models (modified from McMahon et al. 2008b). *EP* exponential piston flow; *DM* dispersion; *E* exponential; *BEP* binary model with piston-flow component and exponential component; *L* linear; *BPP* binary model with two piston-flow components; *SF₆* sulfur hexafluoride; *³H* tritium; *³H(0)* initial tritium; *CFC-11* trichlorofluoromethane

Location (see Fig. 1)	Hydrogeologic setting	Year of construction	Average pumping rate (m ³ /day)	Unsaturated zone thickness (m)	Aquifer saturated thickness in study area (m)	Screened or open interval (m below water table)	Lumped-parameter models (LPMs) applied	Tracers used to calibrate LPMs
Modesto, California (CA)	Unconsolidated alluvial-fan sediments	1961	3,750	<10	>100	18–111	EP, DM	SF ₆ , ³ H, ³ H/ ³ H(0)
Tampa, Florida (FL)	Semi-confined carbonate rocks (karst); overlain by discontinuous confining unit and unconsolidated sediments	1958	2,690	3	>100	33–50	DM, BEP	SF ₆ , ³ H, ³ H/ ³ H(0)
Woodbury, Connecticut (CT)	Unconsolidated valley-fill sediments	1967	390	4	23	10–14	L, E, EP, DM	SF ₆ , ³ H, ³ H/ ³ H(0)
York, Nebraska (NE)	Layered, confined unconsolidated sediments	1977	1,390	<10	80	33–61	BPP, DM	SF ₆ , CFC-11, ³ H

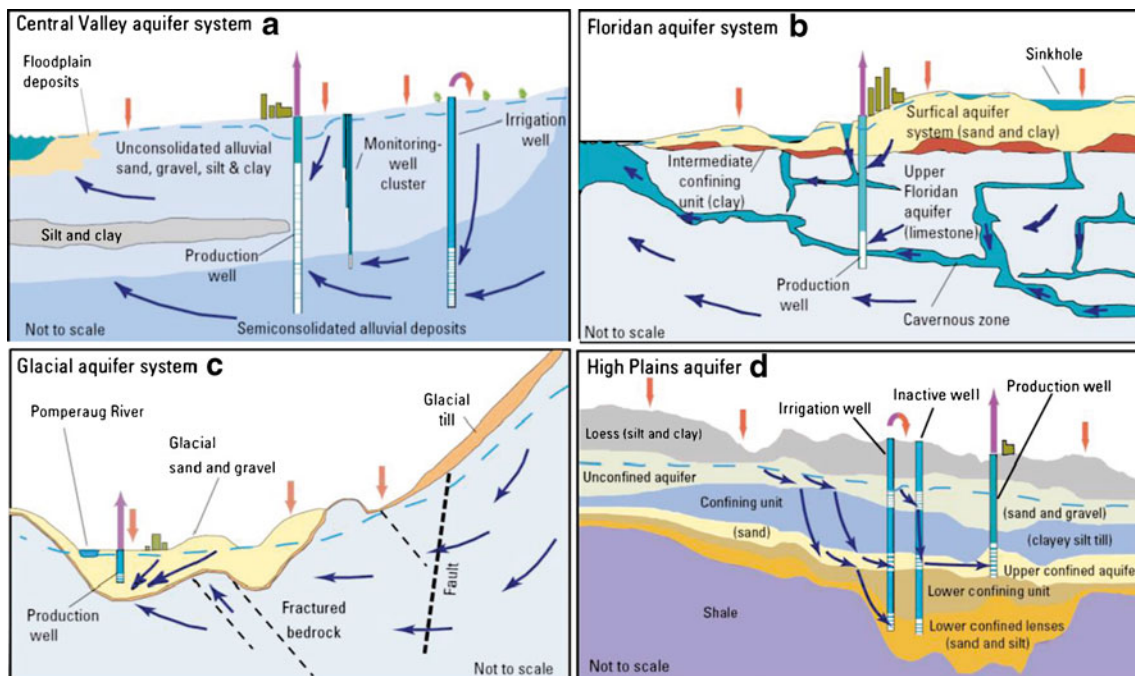


Fig. 2 Conceptual hydrogeologic models of the investigated areas in **a** Modesto, California, **b** Tampa, Florida, **c** Woodbury, Connecticut, and **d** York, Nebraska. *Red arrows*: precipitation (input), *blue arrows*: groundwater flow, *purple arrows*: groundwater abstraction (output), *blue dashed line*: water table. Modified from Landon et al. 2006

The *Woodbury, Connecticut* study area has a humid climate and receives an average of 1,170 mm of precipitation per year. The selected production well is screened in stratified unconsolidated glacial deposits in the Pomperaug River valley (Table 1 and Fig. 2c). The Glacial aquifer system is locally unconfined and depth to water was about 4 m. The unconsolidated valley-fill sediments are underlain by granite, quartzite, schist, and gneiss (Brown et al. 2009; Starn and Brown 2007).

The *York, Nebraska* study area has a humid, continental climate and receives an average of 711 mm of precipitation per year. The selected production well is open to the uppermost confined aquifer in a layered sequence of gravels, sands, silts, and clays (Table 1 and Fig. 2d). The confining unit that separates this aquifer from the overlying unconfined aquifer ranges in thickness from 8 to 17 m and is laterally continuous. Both aquifers are heavily utilized for irrigation, with approximately 2 wells per km², and many irrigation wells are screened across the confining unit. Depth to water in the unconfined aquifer was within 10 m of land surface (Landon et al. 2008; Clark et al. 2007).

Methods

General approach

Geochemical, isotopic, and environmental age tracer data were obtained from the representative drinking-water production well and several nearby short-screened monitoring wells in each study area during 2003–2006. The monitoring-well network in each area was installed in or near the zone of contribution of the selected production

well on the basis of regional-scale (10² to 10³ km²) groundwater-flow models and advective particle tracking (Paschke et al. 2007), incorporating a grid refinement approach (Spitz 2001). Analyzed environmental tracers included various combinations of sulfur hexafluoride (SF₆), chlorofluorocarbons (CFCs), tritium (³H), and tritiogenic helium-3 (³He*), depending on the setting. Because of anticipated effects of wellbore mixing on groundwater age distributions, multiple environmental age tracers were analyzed for each sample, and additional isotopic and chemical data were used to detect reactions and mixing of water masses (Katz et al. 2007; Jurgens et al. 2008; Landon et al. 2008; Brown et al. 2009). Noble gas and nitrogen gas data were used to estimate recharge temperatures and excess air concentrations to convert measured concentrations of the atmospheric environmental tracers in the water samples to concentrations in air for comparison to historical atmospheric concentrations (Plummer et al. 2001). Graphical inspection of data (comparing individual tracers to each other and to simple mixing models) provided initial screening for samples exhibiting tracer contamination or degradation and was used to help select the most appropriate data for inverse modeling of groundwater-age distributions.

Both modeling approaches (particle-tracking and lumped-parameter) were based on the assumption that individual non-reacting environmental tracers and non-point-source contaminants were transported with water molecules (e.g., solutes and solvent were not fractionated from each other by differential diffusion). Therefore, in both model approaches, regardless of the complexity of the hydrologic conceptualization, the concentration of a tracer in a particle was a function of the age of the particle

and the input history of the tracer. The simulated flux-weighted tracer concentration in a mixed sample from a given well at a particular sample date was approximated by a numerical non-parametric version of the convolution integral:

$$C_{s,ts} = \Sigma(X_{i,\tau i} \cdot C_{i,ti} \cdot \exp[-\lambda \cdot \tau i]) \quad (1)$$

where $C_{s,ts}$ is the concentration of a tracer in a sample (s) at the time (date) when the sample was collected for analysis (ts), $X_{i,\tau i}$ is the fraction of the total sample consisting of groundwater with a particular age (τi), $C_{i,ti}$ is the concentration of a tracer in a fraction of the water sample at the time (date) when that fraction entered the system ($ti=ts - \tau i$), λ is a first-order decay constant (zero for a stable tracer), and the sum is over all years represented in the sample ($\Sigma X_{i,\tau i}=1.0$). All particle-tracking and lumped-parameter models were calibrated to tracer data by adjusting selected model parameter values until the best match was achieved between simulated tracer concentrations—derived from computed age distributions using Eq. 1—and measured concentrations for the tracers.

To explore differences between the models and their ability to predict contaminant responses in each production well, computed age distributions were applied to a hypothetical slug input of a conservative contaminant entering the aquifer across the entire area contributing recharge and lasting 25 years. Selected characteristics of the breakthrough curves from the particle-tracking and lumped-parameter models for each well were compared to determine which, if any, of the model differences notably affect contaminant predictions. In addition, results from piston-flow models calibrated to tracer data from each production well were graphed to help illustrate the importance of full age distributions, rather than apparent tracer ages or model mean ages, for trend analysis and forecasting.

Sample collection and data evaluation

Water samples were collected using protocols in Koterba et al. (1995) and analyzed for a broad suite of constituents that could be used to determine water sources and reactions affecting the chemical composition of the groundwater in each setting (Katz et al. 2007; Jurgens et al. 2008; Landon et al. 2008; Brown et al. 2009). Samples from the production wells were collected near the wellhead by means of sample tubing connected to a stainless-steel ball valve that tapped the discharge pipe before the water was chlorinated or treated in any way. Sulfur hexafluoride samples were collected by placing the sampling discharge tubing in the bottom of the sample bottle and displacing the air in the bottle with groundwater. After approximately 2 L of overflow, the sampling line was removed. The bottles were capped with polyseal conical screw-caps without headspace. Chlorofluorocarbon samples were collected by inserting the end of the

discharge tubing into the bottom of a 125-ml glass bottle, allowing at least 2 L to overflow into a 2-L beaker, then capping the sample bottle with an Al foil-lined cap under water within the beaker. Tritium samples were collected in 500-ml bottles for determination by ^3He in-growth. Samples for helium (He) and neon (Ne) analyses and determination of the $^3\text{He}/^4\text{He}$ isotope ratio ($\delta^3\text{He}$) of dissolved He were collected in crimped copper tubes. Samples for additional dissolved gases (N_2 , Ar, CO_2 , CH_4 , O_2) were collected in 160 mL serum bottles, which were sealed in a large beaker under flowing well water.

Concentrations of SF_6 and CFCs were determined at the US Geological Survey (USGS) CFC laboratory in Reston, Virginia, using purge and trap, gas-chromatographic techniques with electron-capture detector (GC-ECD; Busenberg and Plummer 1992, 2000). Concentrations of ^3H , He, Ne, and $^3\text{He}/^4\text{He}$ were determined at the Noble Gas Laboratory of Lamont-Doherty Earth Observatory in Palisades, New York, using methods described in Clark et al. (1976), Bayer et al. (1989), and Solomon et al. (1992). Some ^3H concentrations were determined at the USGS Noble Gas Laboratory in Denver, Colorado, using similar methods. Some major dissolved gas analyses also were obtained from the USGS Noble Gas Lab. These samples were extracted on an ultra-high vacuum extraction line; the extracted gas was analyzed for N_2 , O_2 , CH_4 , and Ar using a quadrupole mass spectrometer in dynamic operation mode. Noble gas isotopic concentrations and compositions were measured using separate aliquots on a magnetic sector mass spectrometer which was run in static operation mode. Concentrations of dissolved gases (N_2 , O_2 , CH_4 , Ar, and CO_2) for all remaining samples were determined at the USGS CFC laboratory by gas chromatography after creation and extraction of headspace in the glass serum bottles (Busenberg et al. 1998).

Recharge temperatures and concentrations of excess air in the groundwater were calculated from the noble gas data according to the closed-system equilibration (CE) model (Aeschbach-Hertig et al. 1999, 2000; Peeters et al. 2002). Where only Ar and N_2 data were available, excess air was assumed to be unfractionated (Heaton and Vogel 1981). For cases where only Ar and N_2 data were available and the sample was anaerobic, the temperature and excess air were assumed to be equal to the average from aerobic samples in the data set for the study area. This was done because of the potential effect of denitrification on the measured N_2 concentration in some of these samples (McMahon et al. 2008a).

Concentrations of SF_6 and CFCs in water samples from the study wells were converted to equilibrium concentrations in air (as dry air mixing ratios, in parts per trillion by volume, pptv) using the calculated recharge temperatures and excess air content for the samples, so that concentrations in the water samples could be compared with historic air mixing ratios for the compounds (Busenberg and Plummer 2000; Plummer and Busenberg 2000). Concentrations of $^3\text{He}^*$ in water samples collected from the study wells were determined from mass balance

equations for ^3He and ^4He , using the measured He, Ne, and $^3\text{He}/^4\text{He}$ ratio for a sample, the calculated recharge temperature, and an assumed $^3\text{He}/^4\text{He}$ ratio of terrigenous He (Schlosser et al. 1989; Solomon et al. 1992; Solomon and Cook 2000). All samples were evaluated for terrigenous sources of He and adjusted accordingly. The concentration of initial ^3H ($^3\text{H}(0)$, tritium concentration before decay) was computed as the concentration of ^3H plus the concentration of $^3\text{He}^*$ in each sample. When comparing simulated concentrations with these measurement-based concentrations, both ^3H and $^3\text{H}(0)$ were simulated as independent tracers (Eq. 1), assuming the decay product ($^3\text{He}^*$) moved with the ^3H in each simulated particle. Subsequently, the ratio of $^3\text{H}/^3\text{H}(0)$ was computed for mixed samples from the simulated values of ^3H and $^3\text{H}(0)$ in the mixtures. Details of the SF_6 , CFC, and $^3\text{He}^*$ calculations as well as an evaluation of the uncertainty associated with the measurements and calculations are given in Katz et al. (2007), Jurgens et al. (2008), Landon et al. (2008), and Brown et al. (2009). The term “measured concentrations” from this point forward implies measurement-based concentrations that have been corrected, converted, or calculated, as discussed in the preceding.

Atmospheric input records for SF_6 and CFCs were obtained from Busenberg and Plummer (2006) and Plummer and Busenberg (2006), respectively. Atmospheric inputs for ^3H were estimated using a computer program (Michel 1989) that interpolates ^3H concentrations from latitude-longitude data in the continental US using measurements from available long-term monitoring stations; records were extended by correlation to International Atomic Energy Agency data from Vienna, Austria (IAEA/WMO 2006).

Differences in unsaturated zone transport of ^3H , which infiltrates as part of the water molecule and decays (“ages”) during unsaturated zone transport, and the gases (SF_6 , CFCs, and He), which pass through the unsaturated zone largely in the gas phase (Cook and Solomon 1995), were not explicitly considered. All of the study areas had unsaturated zone thicknesses of ≤ 10 m and (or) high rates of recharge (discussed in the preceding), such that travel times through the unsaturated zone were considered to be relatively small, and not much larger than the uncertainties of the age distributions for the wells.

Distributed-parameter groundwater-flow models with particle tracking

Steady state, local-scale ($< 15 \text{ km}^2$) three-dimensional groundwater-flow models were constructed for each study area using MODFLOW-2000 (Harbaugh et al. 2000). The USGS particle tracking routine, MODPATH (Pollock 1994), was used to simulate pathlines and advective travel times. Upwards or downwards flow within wellbores (boreholes completed as wells) that were simulated in multiple nodes or layers in the models was tracked by means of the multi-node well package for MODFLOW (Halford and Hanson 2002). A combination of non-linear regression (Hill et al. 2000; Poeter et al. 2005) and trial

and error techniques was employed to calibrate the models to observed water levels, hydraulic gradients, streamflow gains and/or losses, and environmental tracer data from both the monitoring wells and production wells, as described in the following. Calibration of the groundwater-flow models to tracer concentrations was done by applying Eq. 1 using flux-weighted age distributions to generate simulated tracer concentrations for each well for comparison with measured concentrations during error minimization (Clark et al. 2007; Starn and Brown 2007; Burow et al. 2008; Crandall et al. 2009). Flux-weighted age distributions were obtained by delineating the areas contributing recharge to the wells using particles that were captured by the wells during forward tracking. The travel time for each such particle was recorded and the volumetric flux associated with the particle was computed by dividing the total inflow at the model cell face where the particle was started by the total number of particles started at the same cell face. The flux data for all particles related to a given production well were divided into 1-year bins on the basis of simulated travel times to determine the fraction of the total sample consisting of water with a given age in years ($X_{i,ti}$ in Eq. 1).

The *Modesto, California* groundwater-flow model had a uniform grid of 200 rows of 72-m-length cells and 100 columns of 34-m-length cells, and 200 layers with a uniform thickness of 0.6 m, representing the thickness of individual hydrofacies units (Burow et al. 2008). The spatial distribution of the hydrofacies was determined using borehole lithologic data and a three-dimensional spatial correlation model of hydrofacies developed using the program T-PROGS (Carle et al. 1998; Carle 1999). The steady-state model simulated aquifer stresses that existed in water year 2000 and included pumping at 22 production wells. A preliminary calibration was carried out using the parameter estimation process in MODFLOW-2000 (Hill et al. 2000). Because of difficulty updating hydraulic-conductivity-weighted flux boundaries during each parameter estimation run, and because of parameter correlation, estimates for the hydraulic conductivity parameters were later refined using a systematic manual-calibration approach. Observations included water levels measured in 18 monitoring wells screened at multiple depths from 2003 to 2005. Longer-term water-level and pumping data indicated that climatic conditions did not change significantly between 2000 (when the pumping data were collected) and 2005 (when the last of the water-level data were collected). Measured SF_6 concentrations in 8 wells and ^3H concentrations in 20 wells from October 2003 and November 2004 were used to help calibrate this distributed-parameter model (Burow et al. 2008; Jurgens et al. 2008).

The *Tampa, Florida* groundwater-flow model had a uniform grid of 125-m-length cells (80 rows, 69 columns) and 13 layers of variable thickness (Crandall et al. 2009). The steady-state flow model simulated average annual conditions for calendar year 2000 and included pumping from 77 production wells. Karst features such as closed-basin depressions, preferential flow along fractures, and

conduit features were incorporated into the model using high vertical hydraulic conductivity, high recharge, and low porosity values where such features were identified. Twenty-four hydraulic conductivity, recharge, riverbed/drain conductance, and transport (effective porosity) parameters were used to represent the groundwater-flow system. Seventeen parameters, including hydraulic conductivity, recharge, and effective porosity, were estimated using UCODE (Poeter et al. 2005). Observations included groundwater levels from 30 monitoring wells and the production well, hydraulic gradients from 22 monitoring well nests, and measured concentrations of SF₆ and ³H from 17 monitoring wells and the production well. The environmental tracer data used to help calibrate this distributed-parameter model were collected between December 2003 and August 2005 (Katz et al. 2007; Crandall et al. 2009).

The *Woodbury, Connecticut* groundwater-flow model had a uniform grid of 15.2-m-length cells (241 rows, 322 columns), 7 layers of variable thickness, and simulated average annual conditions approximated during 1997–2001, including pumping at five production wells (Starn and Brown 2007). Model parameter values were estimated using the parameter estimation process in MODFLOW-2000. Observations included water levels in 34 monitoring wells and estimates of streamflow gains and/or losses from streamflow data. Simulated travel times were compared to piston-flow model ³H/³He ages (as opposed to tracer concentrations) for 13 of the monitoring wells and the production well; apparent ³H/³He ages were less affected by mixing at this site than at the other sites because the age of nearly all groundwater at the Woodbury site was relatively young (generally <10 years), and the well screens were relatively short (< 4 m in length). In addition, simulated and measured ³H concentrations were compared for the production well. The environmental tracer data used to help calibrate this distributed-parameter model were collected between November 2003 and August 2004 (Starn and Brown 2007; Brown et al. 2009).

The *York, Nebraska* groundwater-flow model had a uniform grid of 40.2-m-length cells (180 rows, 372 columns) and 14 layers of variable thickness (Clark et al. 2007). A transient model that simulated groundwater flow for a 60-year period and included pumping from 183 production wells was initially constructed and manually calibrated to 470 water-level measurements from 53 wells. A transport model within a sub-grid of the groundwater flow model was created with MODFLOW-GWT (Konikow et al. 1996; Konikow and Hornberger 2006) and used to refine the model calibration. Parameter values (horizontal hydraulic conductivity, vertical anisotropy, specific yield, specific storage, porosity) were manually adjusted to minimize differences between groundwater ages computed using the transport model following methods by Goode (1996) and apparent (piston-flow model) ³H/³He and CFC-11 ages for unconfined aquifer monitoring wells with short screens. Simulated CFC-11 concentrations for confined aquifer monitoring wells and the production well were compared to measured concentrations for the same wells.

The simulated CFC-11 concentrations were computed using a steady-state model representing average annual stresses for the period 1997–2001, which was derived from the transient model. The environmental tracer data used to help calibrate this distributed-parameter model were collected between October 2003 and October 2005 (Clark et al. 2007; Landon et al. 2008).

Lumped-parameter models

Steady-state lumped-parameter models (LPMs) were used to describe measured tracer concentrations in each study area. The lumped-parameter modeling approach applied herein was fundamentally similar to the particle-tracking approach except that values of X_{i,τ_i} in Eq. (1) were computed from conceptually relevant weighting functions (analytic age-distribution models) rather than being derived from collections of simulated particles and their transit times. An important difference between the approaches is that the lumped-parameter models treated the flow system as a whole, or as relatively few discrete components, and were calibrated using only environmental tracer data from the production well of interest, whereas the particle-tracking models included spatial variations in aquifer hydraulic and chemical properties and were calibrated using multiple types of data from the production well and monitoring wells.

The weighting functions for the linear model (L), the exponential model (E), the exponential piston-flow model (EP), and the dispersion model (DM) that were applied in this study are presented in Maloszewski and Zuber (1982). The L model is relevant for production wells completed in an unconfined wedge-shaped aquifer or other situations in which age increases linearly with depth. Mean age of the mixed sample (τ_s , subsequently referred to as τ or tau) is the only model parameter. The E model is relevant for production wells in which the shortest flowpath has a travel time equal to zero, the longest has a travel time equal to infinity, and the intervening flowpaths have travel times that are distributed exponentially (decreasing X_{i,τ_i} from young to old). Mean age of the sample (τ) is the only model parameter. In the EP model, the aquifer is assumed to consist of two components of groundwater flow in series, one component described by the exponential model (E) and another component described by the piston-flow model (P) in which all flowpaths are assumed to have the same travel time. The EP model can be used to describe discharge from an aquifer of constant thickness with an upgradient unconfined portion receiving areally distributed recharge (the E part) connected to a downgradient confined portion or an unconfined portion receiving little to no recharge (the P part). Parameter values are the mean age of the sample (τ) and a ratio that describes the relative contributions of the P and E components to the overall mean age, xP/xE , where xE could be equal to the horizontal distance along the flowpath contributing to recharge and xP the horizontal distance along the flowpath not receiving recharge (Cook and Böhlke 2000). The EP model can also be used to describe the age mixture at a well in which the screened interval does not

extend all the way up to the water table and the youngest part of an exponential age distribution in the surrounding aquifer is not sampled by the well. For a well screened from the bottom of the aquifer up to an arbitrary depth below the water table, the parameter xP/xE can be replaced by an expression relating the relative heights of the screened and unscreened portions of the well (assuming the aquifer has an exponential age distribution) (Vogel 1967; Cook and Böhlke 2000):

$$xP/xE = -\ln(1 - z/Z) \quad (2)$$

where z is the distance from the water table to the top of the screened interval and Z is the total saturated thickness of the aquifer. The DM model approximates the age distribution caused by longitudinal dispersion where groundwater particles with different travel times coexist in close proximity. Parameters for this model include mean age (τ) and a dispersion parameter (D').

The binary mixing models used in this study describe situations in which two different water masses from parallel reservoirs mix in a production well. The first binary mixing model (BPP) describes mixing between two components with discrete ages and tracer concentrations. In this study, the BPP model was applied to situations in which relatively young tracer-bearing water with a discrete age mixed with relatively old, tracer-free water. Independent parameters for the BPP model are the mean age of the mixture (τ), the age of the young component, and the age of the old component. The age of the old component was fixed at 60 years to represent tracer-free water. Consequently, the mean age of the mixture is a minimum value as the true age of any tracer-free component is not known and could be large. In contrast, the mean age of the young component and the fractional contribution of this component are meaningful. The second binary mixing model (BEP) describes mixing between a component with an exponential distribution of ages (E) and a component with a discrete age (P) that is younger than that of the exponential component. In this study, the BEP model was applied to a karst situation in which very young water that travels along conduit features mixes in a production well with water from the rock matrix. Parameters for the BEP model are mean age of the mixture (τ), mean age of the exponential component, and age of the piston-flow component.

The Excel workbook TRACERMODEL1 (Böhlke 2006) was updated to include the DM, BPP and BEP models and used to solve Eq. (1) for each model that was evaluated for a given production well. After models with conceptual relevance to the production well and local hydrogeologic setting were selected for comparison, a multi-step approach was used to estimate the model parameter values. Initial parameter values were determined by comparing measured tracer concentrations with concentrations corresponding to model age distributions on tracer-tracer graphs (where curves indicate all combinations of tracer concentrations consistent with a given model type but varying mean age) and tracer-time graphs

(where curves indicate concentrations of individual tracers in a well over time, for a given model type and mean age). Initial values for parameters that affect the plotting positions of model curves on tracer-tracer graphs (e.g., D' for DM; and τ of both components for BPP and BEP) were determined first, by manually adjusting parameter values to obtain a match between the model curve and the tracer data for the production well. For the xP/xE parameter of the EP model, which also affects the plotting position of model curves on tracer-tracer graphs, initial values were determined in some cases using information on the screened and unscreened portions of the well (e.g., Modesto, using Eq. 2, as described in the Results and discussion section in the following). Initial values for parameters that do not affect plotting position on tracer-tracer graphs but do affect plotting position on tracer-time graphs (e.g., τ for E, EP and DM) were then selected in a similar way. Finally, Excel Solver (Fylstra et al. 1998) was used to optimize the parameter values for each model by minimizing the mean absolute percentage error (MAPE) of measured and simulated tracer concentrations. This error function assigns an equal weight to each tracer so that tracers with different units were not preferentially optimized:

$$MAPE = \frac{1}{n} \sum_{i=1}^n \left| 100 \left(\frac{M_i - S_i}{M_i} \right) \right| \quad (3)$$

where M_i is the measured value, S_i is the simulated value, and n is the number of tracers used in the fit. Careful selection of initial parameter values, and multiple trials, were used to avoid local minima. A new Excel workbook, TracerLPM (Jurgens BC, Böhlke JK, Eberts SM, US Geological Survey, unpublished report “TracerLPM: An Excel® Workbook for interpreting groundwater age from environmental tracers”, 2011), also was applied and gave similar results.

Because the production wells were sampled more than once (Table 2), dates for model curves plotted on tracer-tracer graphs (see electronic supplementary material ESM) were calculated for average sample dates at each site (typically $\pm 1-2$ years), although curves for all sample dates were created and evaluated. Tracer-time graphs (ESM) were used to compare measured tracer concentrations with simulated concentrations from both lumped-parameter and particle-tracking models for each production well and sampling date.

Results and discussion

Modesto, California, unconsolidated alluvial-fan sediments

Modesto inverse models

Tracer data and model results for the Modesto site are summarized in Tables 2 and 3, Fig. 3a, and ESM figures 1 and 2 in the electronic supplementary material (ESM). The long screened interval of the Modesto production well

Table 2 Environmental tracer data for samples from selected production wells. Data for Modesto, Tampa, Woodbury, and York prior to 2006 from Jurgens et al. (2008), Katz et al. (2007), Brown et al. (2009), and Landon et al. (2008), respectively (*ND* no data)

Sample date	Sulfur hexafluoride SF ₆ (pptv ^a)	Trichlorofluoromethane CFC-11 (pptv)	Tritium ³ H (TU ^b)	Tritiogenic helium-3 ³ He* (TU)	Initial tritium ^c ³ H(0) (TU)	Tritium/ initial tritium ³ H/ ³ H(0)
Modesto, California						
Nov-2003	ND	ND	6.88 ^d	41.40 ^d	48.28 ^d	0.14 ^d
Aug-2004	0.73	ND	4.57	32.70 ^d	37.27 ^d	0.12
Aug-2006	0.88	ND	ND	ND	ND	ND
Tampa, Florida						
Jan-2004	ND	ND	2.21	ND	ND	ND
Oct-2004	ND	ND	2.10	0.36 ^d	2.46 ^d	0.85
Aug-2005	3.81	ND	2.17	ND	ND	ND
Jul-2006	5.40	ND	2.01	0.56 ^d	2.57 ^d	0.78
Woodbury, Connecticut						
Dec-2003	4.76	ND	6.76	2.98 ^d	9.74 ^d	0.69
Aug-2004	4.43	ND	6.80	2.46 ^d	9.26 ^d	0.73
Jul-2006	5.44	199.0 ^d	ND	ND	ND	ND
York, Nebraska						
Oct-2003	0.24	38.1	0.60	ND	ND	ND
Jun-2004	0.27	ND	0.61	110.79 ^d	111.40 ^d	0.01 ^d
Aug-2006	0.30	48.8	ND	ND	ND	ND

^a Parts per trillion by volume. Concentrations corrected for excess air

^b Tritium unit

^c $^3\text{H} + ^3\text{He}^*$

^d Data not used for lumped-parameter model calibration

(> 90 m) combined with strong, downward hydraulic gradients within the aquifer (up to 0.3) resulted in downward flow of water within the well when it was not pumping. Evidence for this downward movement of water included seasonal fluctuations in nitrate and uranium concentrations in the well, which occurred because shallow contaminated water moved into deeper parts of the aquifer near the wellbore during periods of low or no pumping and subsequently was pulled back out when pumping resumed (greatest during winter months when down time between pumping events was longest) (Burow et al. 2008; Jurgens et al. 2008). This intra-wellbore flow had the potential to affect concentrations of environmental tracers and, to a lesser extent, ratios of tracers. Thus, data collected during the summer pumping season were most representative of the surrounding aquifer system (Table 2) and the timing of tracer data collection was a consideration for estimating the age distribution of water from this well.

Lumped-parameter models applied to the Modesto site included the EP and DM models. For the EP model, the initial estimate of the xP/xE parameter (0.18) was computed from the length of the saturated cased interval below the water table (18 m) and the total length of the well including the screened interval (111 m) using Eq. 2. For the DM model, the initial estimate for the D' parameter was obtained by adjusting the parameter value until the model curve best matched the selected tracer data on tracer-tracer graphs (see ESM figure 1, ESM). The final EP ($\tau=54$; $xP/xE=0.2$) and DM ($\tau=59$; $D'=0.51$) models were both conceptually feasible and reproduced the production-well tracer data from August 2004 and August 2006—times when the effects of intra-wellbore flow on tracer concentrations were likely to be minimal (see ESM figures 1 and 2, ESM).

Water samples from the Modesto well had a wide range of ages minus the youngest fraction that was missing because the top of the well screen was 18 m below the water table. The particle-tracking model yielded an age range for the well of 9 years to more than 1,000 years. The simulated peak in the age distribution from this model was around 25 years (Fig. 3a) (Burow et al. 2008). Graphs of ³H versus ³H/³H(0) and of SF₆ versus ³H/³H(0) confirm that the water from the production well is of mixed age—the tracer data plot off curves that describe no mixing (see ESM figure 1, ESM). This was not unexpected for the production well because of its long screened interval. The same was also true, however, for samples from nearby monitoring wells (1.5-m screened intervals), which is consistent with other modeling studies indicating aquifer heterogeneity can affect apparent SF₆ ages in short-screen wells in the California Central Valley (Weissmann et al. 2002; Green et al. 2010). The large difference between the mean age calculated using the particle-tracking model (420 years) and the mean ages calculated using the two lumped-parameter models (54 and 59 years) illustrates how small numbers of very old particles can influence the mean age computed from particle-tracking results. The median age from the particle-tracking was 46 years.

Modesto contaminant predictions

Breakthrough curves for the Modesto production well based on the age distributions from each of the calibrated models and a hypothetical nonpoint-source contaminant with a uniform input at the water table lasting 25 years and without degradation are plotted on Fig. 4a and further characterized in Table 3. The particle-tracking model predicted a maximum relative concentration of 0.43,

Table 3 Model parameter values and breakthrough-curve characteristics at production wells for a hypothetical contaminant with a uniform slug input at the water table lasting 25 years and no degradation. Median age, peak lag time, dilution at peak, arrival: 1% of total mass, and flush: 99% of total mass for Particle-Tracking Models are from McMahon et al. (2008b) (*EP* exponential piston-flow model; *DM* dispersion model; *BEP* binary model with piston-flow component and exponential component; *L* linear model; *E* exponential model; *BPP* binary model with two piston-flow components; *PTM* particle-tracking model)

Model	Mean absolute percentage error (%)	Peak lag time ^a (years)	Dilution at peak (C/C _o) ^b	Arrival: 1% of total mass ^c (years)	Flush: 99% of total mass ^d (years)	Time to breach 10% of input concentration ^e (C/C _o =0.1) (years)	Time to return to below 10% of input concentration ^e (C/C _o =0.1) (years)	Time above 10% of input concentration (C/C _o =0.1) (years)
Modesto, California								
EP tau ^e =54 years, xP/xE=0.2	7.5	20	0.43	14	205	13	99	86
DM ^f tau=59 years, D'=0.51	7.6	22	0.40	14	275	14	94	80
PTM mean age=420 years, median age=46 years	19.5 ^g	26	0.43	17	216	18	78	60
Tampa, Florida								
DM ^h tau=6 years, D'=1.06	14.7	12	1.00	2	30	<1	37	37
DM ⁱ tau=18 years, D'=2.24	0.3	12	0.82	2	164	1	48	47
BEP ^h tau=7 years, old (E) tau=25 years, young (P)=0.5 years, % young (P)=72	10.2	12	0.99	1	16	<1	32	32
BEP ⁱ tau=18 years, old (E) tau=25 years, young (P)=0.5 years, % young (P)=29	9.2	12	0.82	1	68	<1	55	55
PTM mean age=15 years, median age=13 years	41.8 ^g	12	0.76	2	61	<1	60	60
Woodbury, Connecticut								
L tau=6 years	4.5	<1	1.00	2	9	1	35	34
E tau=5 years	4.1	12	1.00	2	13	<1	35	35
EP tau=5 years, xP/xE=2.8	4.2	11	1.00	5	7	4	32	28
DM tau=5 years, D'=0.37	3.3	12	0.98	3	14	1	35	34
PTM mean age=6 years, median age=7 years	5.0 ^g	6	1.00	3	8	1	33	32
York, Nebraska								
BPP old (P) tau≥60 years, young (P)=21 years, % young (P)=15	10.0	21 ^j	0.15 ^j	21	≥60	21	46 ^j	25 ^j
DM tau=180 years, D'=1.12	66.0	28	0.21	18	322	23	98	75
PTM mean age=186 years, median age=80 years	222.0 ^g	30	0.20	18	359	25	122	97

^a Time lag between input midpoint of 12.5 years and first occurrence of peak concentration

^b Concentration relative to input concentration

^c Time relative to start of input

^d Time relative to end of input

^e tau refers to mean age

^f Dispersion model parameters follow Maloszewski and Zuber (1982)

^g Mean absolute percentage error for PTMs computed from measured and simulated tracer concentrations at the production well for comparison purposes only. PTMs were calibrated to a variety of distributed data, including water levels, hydraulic gradients, streamflow gains and/or losses, and environmental tracer data for both monitoring wells and production wells. Consequently, tracer data for individual production wells have less influence on PTM model calibration than they do on lumped-parameter model calibration

^h Calibrated to data from January 2004, October 2004, August 2005, and July 2006

ⁱ Calibrated to data from August 2005

^j Young fraction only

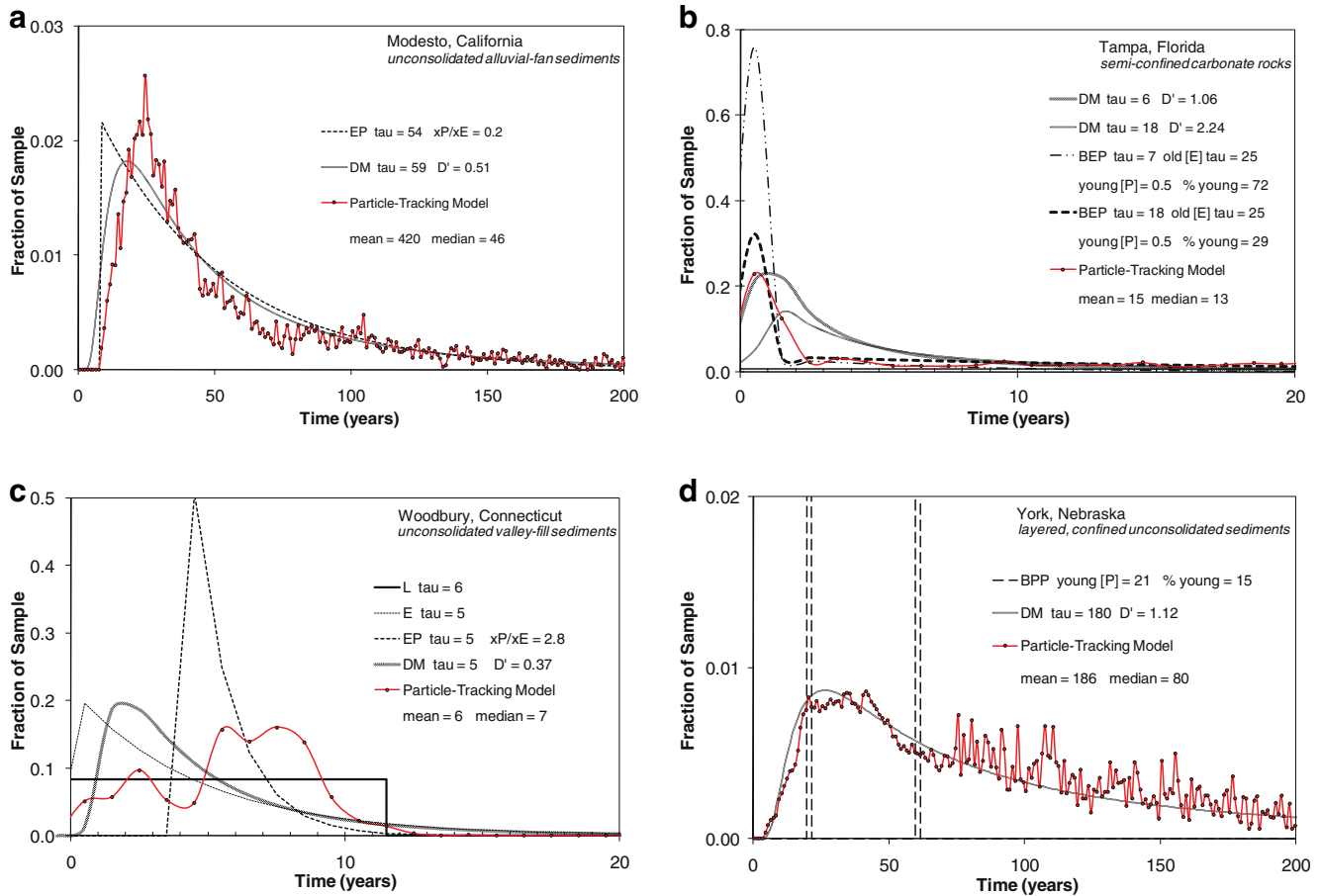


Fig. 3 Simulated groundwater-age distributions for **a** Modesto, **b** Tampa, **c** Woodbury, and **d** York. Individual curves correspond to different models, where *L* is linear, *E* is exponential, *EP* is exponential piston flow, *DM* is dispersion, *BEP* is binary exponential and piston-flow mix, *BPP* is binary piston flow and tracer-free mix, and *Particle-Tracking Model* is three-dimensional groundwater-flow model with particle tracking. Note that the *y*-axis scales are different in **a–d** and that the *x*-axis scales in **b** and **c** differ from those in **a** and **d**

whereas the maximum relative concentration would have been 1.0 had there been no mixing (P model). The EP and DM predicted maximum relative concentrations of 0.43 and 0.40, respectively. Both the EP and DM models predicted the arrival of the first 1% of total mass at the well within 3 years of the particle tracking predictions. An important feature of the EP, DM and particle-tracking models is the delay before contaminant arrival and recovery caused by the lack of young water, owing to the distance between the water table and the top of the well screen. The models all predict somewhat different flushing times for the last 1% of total mass and different amounts of time above a threshold concentration equal to 10% of the input concentration (relative concentration of 0.1; Table 3). The small fraction of water produced by this well that is young enough to contain the selected age tracers contributes to the relatively large uncertainties in the tail end of the age distributions from the fitted models (Zuber et al. 2005; Chorco Alvarado et al. 2007). Had tracers of much older groundwater such as carbon-14 or ⁴He, been included in the analysis, the tail end of the age distribution may have been better constrained. Nevertheless, all mixing models predict that concentrations would remain above a relative concentration of 0.1 for decades longer than the 25 years of the slug input.

Tampa, Florida, semi-confined carbonate rocks (karst)

Tampa inverse models

Tracer data and model results for the Tampa site are summarized in Tables 2 and 3, Fig. 3b, and ESM figures 3 and 4 (ESM). Karst features enabled surficial aquifer system (SAS) water to short-circuit the intermediate confining unit (ICU) and rapidly reach the production well in the Upper Floridan aquifer (UFA; Stewart et al. 1978; Katz et al. 2007). Evidence indicating hydraulic short-circuiting included concentrations of natural compounds (radon-222, uranium, arsenic, dissolved organic carbon, and hydrogen sulfide) in water from the production well that were intermediate between concentrations in water from SAS and relatively isolated UFA monitoring wells, along with concentrations of anthropogenic compounds (nitrate, volatile organic compounds, and pesticides) that were closer to those found in SAS monitoring wells. Thus, hydraulic short-circuiting by means of karst features was a consideration for estimating the age distribution of water from this well.

Lumped-parameter models applied to this well included the DM and BEP models. The DM model was thought to be

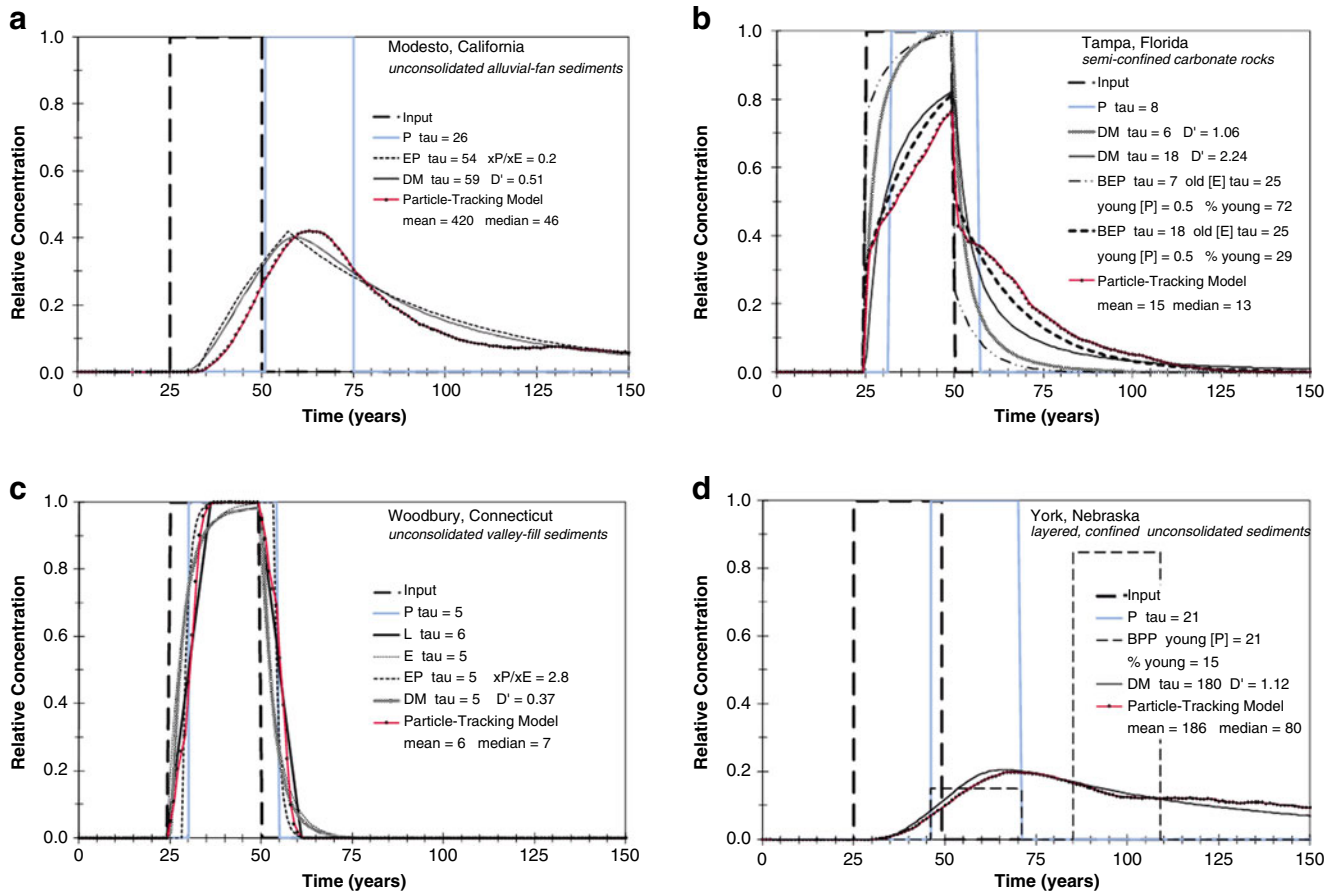


Fig. 4 Relative concentration of a hypothetical contaminant in a production well in **a** Modesto, **b** Tampa, **c** Woodbury, and **d** York as a function of time resulting from a uniform slug input at the water table across the area contributing recharge lasting 25 years (from time 25 years to time 50 years) and no degradation. Individual curves correspond to different models, where *P* is piston flow (no mixing), *L* is linear, *E* is exponential, *EP* is exponential piston flow, *DM* is dispersion, *BEP* is binary exponential and piston-flow mix, *BPP* is binary piston flow and tracer-free mix, and *Particle-Tracking Model* is three-dimensional groundwater-flow model with particle tracking

potentially relevant because karst features can result in macro-dispersion within an aquifer. The BEP model also was considered to be conceptually feasible because of geochemical evidence indicating that the production well produced a mixture of SAS water and UFA water, which would not have had a single, discrete age. The discrete age for the young component of the BEP model was not obvious on tracer-tracer graphs because of the generally young age of water in the mixture (see ESM figure 3, ESM). Rather, the age of the young component was assumed to be less than 1 year to represent rapid movement of water along karst features in response to the large pumping stress (2,690 m³/day) imposed by the well. Evidence of such rapid movement of water included differences in the chemical composition of the water from the production well under ambient and pumping conditions and historic detections of fecal streptococci in wells within the wellfield (Katz et al. 2007; Stewart et al. 1978). The lumped-parameter models were calibrated using the complete tracer data set (Table 2), and with a subset of the data from the August 2005 sampling, as discussed in the following.

Water from the Tampa production well had simulated particle ages ranging from less than 1 year to more than

100 years. The peak in the age distribution from the particle-tracking model was less than 1 year (Fig. 3b). The youngest water to arrive at the production well in the particle-tracking model followed karst features (Crandall et al. 2009). The tracer data also showed the effects of hydraulic short-circuiting as a result of karst features. Samples from the production well—open solely to the UFA—were more similar to samples from SAS monitoring wells than to most UFA monitoring wells on graphs of ³H versus ³H/³H(0) and ³H versus SF₆ (see ESM figure 3, ESM). Tracer-time graphs revealed that none of the models were capable of describing the complete tracer data set from this production well, including the particle-tracking model (see ESM figure 4, ESM). However, He data were not used to help calibrate the particle-tracking model because a graph of SF₆ versus ³H/³H(0) indicated possible ³He* loss in some early samples from the production well and several SAS monitoring wells (Katz et al. 2007). As a result, the lumped-parameter models were calibrated a second time using just the subset of tracer data used to help calibrate the particle-tracking model (SF₆ and ³H concentrations from August 2005) in order to facilitate a comparison of the simulated responses (Table 3).

Tampa contaminant predictions

Hypothetical contaminant breakthrough curves for all models for the Tampa production well are summarized in Fig. 4b and Table 3. The curve for the BEP model that was calibrated to the August 2005 tracer data ($\tau=18$ years; old (E) $\tau=25$ years; young (P) $\tau=0.5$ years; % young (P)=29) was most similar to that of the particle-tracking model. Both this BEP model and the particle-tracking model produced curves with an initial rapid response to changes in contaminant loading, followed by a slower response. In addition, both predicted a maximum relative concentration of approximately 0.8 and concentrations above 10% of the input concentration (relative concentration of 0.1) lasting between 55 and 60 years. The age distributions from both models were consistent with the larger geochemical data set, as well as results of several other geochemical mixing models (Katz et al. 2007). The DM model that was calibrated to August 2005 tracer data ($\tau=18$ years, $D'=2.24$) also predicted a maximum relative concentration of approximately 0.8, but it predicted concentrations above a relative concentration of 0.1 lasting for a shorter period of time (47 years). Moreover, this DM model indicated that the fraction of very young water (< 1 year) was close to 5%, whereas the BEP and particle-tracking models (calibrated using the same tracer data) indicated that the very young fraction was above 20% (Fig. 3b). The close similarity in the breakthrough curves for the BEP model (calibrated to the August 2005 data) and the particle-tracking model was an outcome of the similarity in the conceptual model that served as the foundation for both models and the tracer data that were used to help calibrate the models. The BEP model that was calibrated using the complete data set simulated the same conceptual model but suggested a larger contribution of very young water (Fig. 3b). The age distribution at this well completed in a karst aquifer may be relatively variable and may not be properly represented under varying flow conditions by any of the steady-state models (e.g., Ozyurt and Bayari 2005).

Woodbury, Connecticut, unconfined valley-fill sediments (glacial deposits)

Woodbury inverse models

Tracer data and model results for the Woodbury site are summarized in Tables 2 and 3, Fig. 3c, and ESM figures 5 and 6 (ESM). Groundwater in this relatively small, unconsolidated valley-fill aquifer is relatively young. Piston flow model (apparent) groundwater ages for monitoring wells throughout the valley were generally < 10 years (Brown et al. 2009). This young water in combination with the short-screened interval of the production well (4 m, near the vertical center of the total saturated thickness of 23 m) resulted in a groundwater age range that was relatively narrow compared to the other production wells in the study. Tracer-tracer graphs indicated the local bedrock may have served as a terrigenous source of SF₆ (see ESM figure 5, ESM). While most monitoring wells were completed in the unconsolidated

sediment, one bedrock monitoring well had an SF₆ concentration just above 30 pptv (off-scale on graphs). Excess (terrigenous) SF₆ appeared to affect monitoring well samples more than samples from the production well. Differences in the occurrence of excess SF₆ in waters from the different types of wells may have occurred because of the relatively rapid throughput of water within the zone of contribution of the production well compared to that of the monitoring wells, minimizing the accumulation of terrigenous SF₆ in water from the production well. Plummer et al. (2001) observed that rapid throughput of water to springs in a setting with a terrigenous SF₆ source minimized the accumulation of SF₆ in the spring water. Concentrations of CFCs were generally greater than atmospheric equilibrium values and were not useful for estimating the age distribution at the production well.

Lumped-parameter models applied to this well included the L, E, EP and DM. Curves for the various lumped-parameter models were generally indistinguishable in the vicinity of the tracer data on the tracer-tracer and tracer-time graphs (see ESM figures 5 and 6, ESM). This is primarily because the water was relatively young and the well screen was relatively short in comparison to the aquifer thickness. As a result, visual inspection of tracer-tracer graphs did not provide much information for resolving which model was more likely to represent the age distribution in the well. Nevertheless, for a given model type, the tracer-time graphs were useful for constraining model parameter values (e.g., E model in ESM figure 6, ESM). Optimal parameter values for each lumped parameter model (Table 3) were obtained by calibrating to the SF₆, ³H and ³H/³H(0) data for the production well (Table 2).

The Woodbury production well was the only one considered in this study that did not produce any water > 60 years of age according to any of the models. The particle-tracking model yielded a mean age of 6 years and a range of ages from less than 1 year to approximately 15 years in the production well. Although the well screen was short, the particle age distribution for the well was relatively broad and weakly bimodal because of variations in the recharge rate across the contributing area for the well, which resulted from variations in the hydraulic properties of the subsurface material (Starn and Brown 2007; Fig. 3c). The L model produced the age distribution most similar to that from the particle-tracking model, but did not describe the bimodal distribution derived from particle tracking, as it did not account for spatial variations in aquifer hydraulic properties.

Woodbury contaminant predictions

Breakthrough curves for the hypothetical contaminant pulse at the Woodbury well are shown in Fig. 4c. Selected characteristics of the curves are listed in Table 3. The breakthrough curves for the particle-tracking model and all lumped-parameter models, including the P model, are relatively similar to each other for this well. This is because of the young age of the water combined with the relatively narrow age range.

York, Nebraska, layered, confined unconsolidated sediments

York inverse models

Tracer data and model results for the York site are summarized in Tables 2 and 3, Fig. 3d, and ESM figures 7 and 8 (ESM). This site was difficult to interpret because of anthropogenic modifications to the flow system, primarily associated with irrigated agriculture, and the lack of ideal tracers. Stable isotope data ($\delta^{18}\text{O}$ and δD) revealed that the production well, which was completed in a confined aquifer, and some confined-aquifer monitoring wells produced mixtures of confined and unconfined aquifer water. The non-uniform distribution of mixed waters from wells in the confined aquifer indicated that there were preferential flowpaths across the confining unit separating the two aquifers (Landon et al. 2008). The three-dimensional particle-tracking model indicated that nearly 25% of the water in the confined aquifer entered the aquifer along wellbores or annular spaces of irrigation, commercial, or older production wells that were constructed across the overlying confining unit (Clark et al. 2007; Landon et al. 2008).

Tracer-tracer graphs indicated a possible source of terrigenous SF_6 that affected monitoring well samples more than samples from the production well (ESM figure 7, ESM) and may be related to granite-derived sediments in the study area. Concentrations of CFC-12 in nearly half of the monitoring wells (confined and unconfined) were greater than atmospheric equilibrium values, pointing to a local source of CFC-12. The CFC-11 data did not show similar signs of contamination and were widely available for the study area. Some monitoring well samples from the confined aquifer had detectable concentrations of atmospheric gas tracers (SF_6 and CFCs) but were free or nearly free of ^3H —a combination that may have resulted from irrigation with ^3H free water from confined parts of the aquifer system. In addition, samples from the production well had high concentrations of terrigenous ^4He (> 90% of total He), making the He data for the well unusable for age estimation. Thus, the lumped-parameter models were calibrated to SF_6 , CFC-11, and ^3H data (Table 2), as well as to a subset of the data that did not include the ^3H values, because of the potential effect of irrigation with ^3H free water on ^3H concentrations at the production well.

Lumped-parameter models applied to this study area included the BPP and DM models. Comparison of the tracer data and curves for the calibrated models on tracer-tracer and tracer-time plots revealed that the BPP model (old (P) $\tau \geq 60$ years; young (P) $\tau = 21$ years; % young (P) = 15) best described the complete tracer data set for the production well (ESM figures 7 and 8, ESM). Recalibration of the BPP model without the ^3H data produced essentially the same age mixture for the well. Although the BPP model cannot be exactly correct because the model assigns a single age to the young component and the young water from the unconfined aquifer must have had a range of ages, these results indicate that the young component was likely derived from deeper parts of the unconfined aquifer. The DM model was potentially

consistent with a conceptual model in which upgradient wells with long-screened intervals served as hydraulic short-circuits across the confining unit. A unique solution for the DM model could not be achieved when the complete data set (SF_6 , CFC-11, and ^3H data) was used for model calibration. The DM model in Table 3 was calibrated to SF_6 and CFC-11 data. An initial value for the D' parameter for this DM model was obtained by adjusting the parameter value until a good visual match between the model curve and the data on a graph of SF_6 versus CFC-11 was achieved.

Water from the York production well had a wide range of ages (Fig. 3d). The particle-tracking model indicated that all young water (< 60 years) in this well—approximately 35% according to the model—entered the confined aquifer by way of upgradient wells completed across the overlying confining unit. The DM model produced an age distribution that was similar to that of the particle-tracking model. However, it could not be used to differentiate the sources of water for the well (water that flowed through the overlying confining unit versus water that short-circuited the confining unit by way of upgradient wellbores). The BPP model had a different age distribution and yielded an estimate of the contribution of young, unconfined aquifer water at 15%. Despite their differences, both the DM model and the BPP model are consistent with the particle tracking results in having little or no very young water, minor fractions of water from relatively deep parts of the unconfined aquifer, and larger fractions of older tracer-free water from the confined aquifer (for which the age distribution is unknown).

York contaminant predictions

Breakthrough curves for the BPP, DM and particle-tracking models are plotted on Fig. 4d and further characterized in Table 3. The breakthrough curve from the DM model matches that of the particle-tracking model. Both models predict a maximum relative concentration close to 0.2, the arrival of 1% of total mass at 18 years, and close to 25 years to exceed 10% of the input concentration (threshold concentration of 0.1 relative to input). The conceptually more simple BPP model predicts a maximum concentration of 0.15 if the old component (≥ 60 years) is not affected, 21 years for the arrival of the first 1% of contaminant mass, and 21 years to breach the threshold concentration. While the predicted time above a relative concentration of 0.1 is notably different for each model, it may be sufficient for some purposes to know that the differing models provide similar information regarding the early response of the production well to contamination.

Utility of age-distribution models for evaluating production well vulnerability

Comparison of modeling approaches

In each of the four investigated settings, both types of models applied in this study (groundwater-flow models with advective particle tracking and lumped-parameter models)

yielded similar age distributions and concentration trends at production wells for real and imaginary tracers, when based on similar conceptual models of local hydrogeology and calibrated to similar tracer measurements (Fig. 5). Although particle-tracking models yielded age distributions with more internal structure, those irregularities did not necessarily cause significant differences in calculated tracer concentration records or contaminant trends in mixed samples from production wells. In some cases, lumped-parameter models based on different conceptual models yielded indistinguishable results when calibrated to the same tracer data; for example, the EP and DM models both have peaks and long tails in their age-frequency distributions, such that parameter values yielding similar concentrations for most tracers over time were attainable. Therefore, in areas with limited local hydrogeologic information, it may be difficult to distinguish these age distribution models, even with multiple environmental tracer data. For the same reason, however, these types of ambiguity may not substantially affect predicted contaminant responses from these models. At the same time, the P model clearly has limited utility for trend analysis and forecasting at the production wells (Fig. 4).

Important differences exist in the ability of the different models to incorporate data from distributed monitoring wells and to provide information about spatial variation in contaminant source areas. In the current study, for example, particle-tracking model calibration was based, in part, on various chemical and isotope data from monitoring-well networks indicating recharge rates, interactions between aquifers, and hydraulic short-circuiting. In principle, lumped-parameter model calibration can yield useful age distributions for production wells in the absence of distributed tracer data in the aquifer if production-well data are available for a single tracer collected over an extended period of time (ideally decades) or for an array of independent tracers collected simultaneously, but such data may be difficult to obtain. In practice, ancillary data (e.g., geologic sections and well construction data, other chemical and isotopic data collected with the environmental tracers, or time-series water quality records for the well) were required in most cases to help formulate a conceptual model and parameterization scheme for the lumped parameter models in this study.

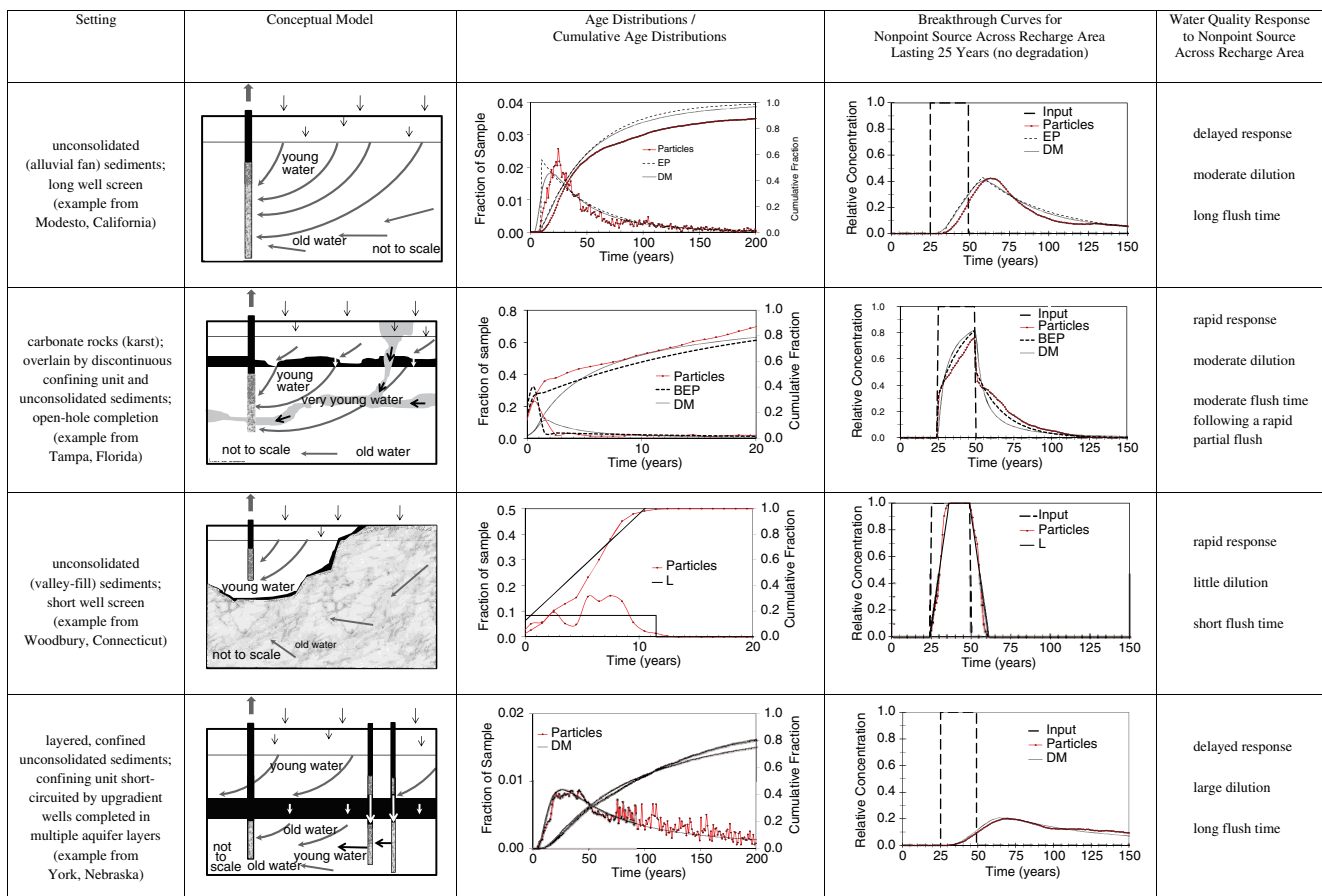


Fig. 5 Summary of age distributions from particle-tracking and conceptually feasible lumped-parameter models that best reproduced selected tracer data representative of the surrounding aquifer, and corresponding information on production-well vulnerability to contamination. *Downward black arrows*: precipitation/recharge (input), *gray arrows*: general direction of groundwater flow, *white arrows*: groundwater flow across confining unit, *heavy black arrows*, groundwater flow associated with hydraulic short-circuit, *upward gray arrows*: groundwater abstraction (output). Individual curves on graphs correspond to different models, where *Particles* is three-dimensional groundwater-flow model with particle tracking, *EP* is exponential piston flow, *DM* is dispersion, *BEP* is binary exponential and piston-flow mix, and *L* is linear

Even well-calibrated lumped-parameter models may be deficient where spatial variations in contaminant source areas are important. For example, in another study related to this one at the Modesto site, the production-well age distribution from the particle-tracking model was coupled with a NO_3^- input function that varied both temporally and spatially based on historic land use (McMahon et al. 2008b). This was done by associating water particles of different ages at the production well with simulated flowpaths linking the well to the land surface in specific capture areas. The simulated production-well response to spatially varying land-use change was different from a simulated response to uniformly changing land use. The lumped-parameter models for this site would not provide similar information on the spatial relation between a well and non-uniform contaminant sources near land surface.

It is also possible that both particle-tracking and lumped-parameter model approaches will be inappropriate in some types of hydrogeologic settings. For example, because both approaches in this study relied on the assumption that tracers move with water particles, both could yield biased results where differential diffusion causes separation of individual dissolved constituents from each other and from water parcels, for example in some dual-porosity karst or fractured rock aquifer systems. In addition, both could yield similar, albeit incorrect results where an assumption of steady-state is applied but transient conditions prevail. Although flow rates through hydrogeologic systems are transient, a steady-state approximation can be applicable to systems in which the volume of water that is variable is small in comparison to the total volume of the system (Zuber 1986; Małozewski and Zuber 1996). While many groundwater systems likely satisfy this condition, some (e.g., karst systems, small basins) may require transient models (e.g., Ozyurt and Bayari 2005). These limitations highlight the importance of the foundational conceptual model, regardless of the model approach.

Relevance to source-water protection and well vulnerability assessments

Estimated age distributions from both the particle-tracking and lumped-parameter models can provide useful information related to source-water protection and well vulnerability assessments. For example, time-of-travel zones often serve as the basis for source-water protection efforts, and flux-weighted age distributions from both model approaches could be used to estimate the percent of water from a well associated with specific time-of-travel zones at the water table. For the wells in this study, the simulated cumulative age distributions (Fig. 5, column *Age Distributions*) point to notable differences in the water-table expression of the 10-year time-of-travel zones. Specifically, greater than 95% of the water produced by the Woodbury well (unconsolidated valley-fill sediments) recharged the aquifer within the previous 10 years. This fraction was less than 5% for the York well (confined unconsolidated sediments) and Modesto well (unconsolidated alluvial fan sediments) and close to

60% for the Tampa well (semi-confined carbonate rocks). Thus, the Woodbury well would respond more readily to activities near the land surface compared with the Modesto and York wells. Conversely, the Modesto and York wells would derive greater benefit from dilution of anthropogenic compounds introduced near the water table from in-well mixing with relatively old, unaffected water.

A simulated age distribution also could be used to estimate a ‘worst-case’ concentration for a well from a period of widespread contaminant input near the water table. In practical terms, the specified period might be chosen to represent the time since a new contaminant was first introduced at the water table. For the scenario simulated in this study in which a hypothetical contaminant was introduced at the water table over 25 years and no degradation was assumed, it might be argued, for example, that a relative concentration of 0.4 at the deep, long-screened-interval Modesto well (alluvial-fan sediments) would reflect the dilution capacity of the well, whereas the same relative concentration at the shallow, short-screened-interval Woodbury well (valley-fill sediments) could be an early indication of greater concentrations to come (Fig. 5, column *Breakthrough Curves*).

Summary

Results from four contrasting hydrogeologic settings illustrate the importance of age distributions (as opposed to model mean ages or apparent tracer ages) for rationalizing and predicting responses of drinking-water production wells to nonpoint sources of contaminants. Differing interactions between production wells and major hydrogeologic features result in differing contaminant trends in such wells, including notably different lag times (time to initial response), dilution factors, and turnover times (buildup or flushing times) (Fig. 5, columns *Breakthrough Curves* and *Water Quality Response*). Because the age distribution of water in such wells affects both the concentrations and trends of chemical constituents in the wells, it is important for information on groundwater-age distributions to be applied more routinely to water-quality issues and to the design of monitoring programs. In order for this to occur, reasonable approximations of groundwater-age distributions must be available for many more wells. A comparison of groundwater-age distributions for production wells derived from detailed three-dimensional groundwater-flow models with advective particle tracking (referred to as particle-tracking models) and lumped-parameter models demonstrates that estimates from the various models can be similar when they are based on similar conceptual hydrogeologic models and calibrated to similar, multiple age-tracer data using inverse methods (Fig. 5, column *Age Distributions*).

For a deep well completed in a thick section (> 90 m) of heterogeneous alluvial fan sediments, EP (exponential piston-flow) and DM (dispersion) lumped-parameter models provided estimates of the age distribution at the well that were similar to each other and to that of a particle-

tracking model. The age distribution from each of the models indicated that a well similar to this one would have an initially delayed response to input of a nonpoint-source contaminant (close to 15 years for arrival of the first 1% of contaminant mass); the concentration at the well would likely be diluted by old, unaffected water due to the wide range of groundwater ages at the well; and it would take many decades for the contaminant to be flushed from the well.

For a well in a carbonate-rock setting, both BEP (binary exponential piston-flow) and particle-tracking models were able to simulate contributions to the well from fast flow in karst features and slower flow through the aquifer matrix. Simulated age distributions and breakthrough curves from these models were similar when similar tracer data were used for model calibration. Both models indicated that a well like this one would respond very rapidly to contaminant input at the water table (1–2 years for arrival of the first 1% of contaminant mass); may benefit from a moderate amount of dilution at the well, depending on the duration of contaminant input (peak concentration around 80% of the input concentration in the scenario simulated in this study); and it could take decades for the concentration at the well to return to unaffected levels. A DM model calibrated to the same tracer data also predicted similar amounts of dilution, as well as decades for contaminants to be flushed from the well. However, the initial response predicted by the DM model was not as rapid as what was predicted by the BEP and particle-tracking models.

For a shallow well with a short-screened interval (4 m) in a valley-fill aquifer, all models that were tested (L, linear; E, exponential; EP; DM; and particle tracking) could be fit reasonably well to the tracer data because the range of ages was small. Likewise, the models yielded roughly similar breakthrough curves at the production well in response to a hypothetical slug input of a nonpoint-source contaminant lasting 25 years despite having different age distributions. For a well similar to this one, the initial response at the well would be rapid (5 years or less for arrival of the first 1% of contaminant mass) and there would be little contaminant dilution at the well (peak concentration around 100% of the input concentration), but the concentration at the well would decrease rapidly following the removal of the contaminant source (less than 15 years to flush 99% of the contaminant mass in the scenario simulated in this study). Differences between the models could be important for describing changes at shorter time scales (e.g., months to years), but other types of environmental tracers (or long-term tracer monitoring) would be required to distinguish the age-distribution models for this well.

For a well in a confined aquifer where the confining unit has been breached by other wells completed in multiple aquifer layers upgradient of the production well, a DM model produced an estimated age distribution similar to that produced by a particle-tracking model. For a well similar to this one, the lag time between contaminant input at the water table and the response at

the well would depend on the proximity of the upgradient wellbore(s) serving as hydraulic short-circuits. Although the well would likely benefit from a large amount of in-well dilution (peak concentration around 20% of the input concentration for the scenario simulated in this study), it could take nearly a century for the contaminant to be flushed from the surrounding aquifer and the well.

Overall, detailed distributed-parameter groundwater-flow models with particle tracking and appropriate lumped-parameter models can be indistinguishable in their ability to reproduce either temporal environmental tracer data or multiple environmental tracer data from individual production wells. Similarly, different models can produce indistinguishable predicted responses to nonpoint-source contaminant input that varies temporally but not spatially. Only the distributed-parameter particle-tracking models provide information on the spatial relation between actual contaminant sources and a well. Age distributions from both types of models can be used to identify (1) wells that are likely to respond quickly to land-use activities and wells that are likely to respond more slowly; (2) wells in which modern anthropogenic contaminants will be more or less diluted by relatively old, unaffected waters (or vice versa, depending on contamination history); (3) wells in which concentrations could remain elevated for many decades regardless of imposed protection measures; and (4) wells that could benefit most from source-protection efforts that seek to manage the movement of contamination-susceptible water locally through well-bores or other short-circuiting features. In contrast, apparent tracer ages (estimated using piston-flow models) and model mean ages cannot provide similar insight into the vulnerability of a production well to nonpoint-source contaminant input.

For any approach used to estimate age distributions in water from a production well, long-term records of tracer concentrations and (or) simultaneous measurements of multiple tracers can reduce uncertainties in model conceptualization and parameterization. However, complications arise when (1) the tracers are affected by chemical or physical processes that cause their concentrations to deviate from their atmospheric input function, or (2) the tracers have similar input functions over the time scale of interest. These difficulties limited some interpretations in this study and may be largely unavoidable in many systems; nevertheless, the implications of age distributions for production well contamination cannot be ignored. Other data besides age tracer concentrations clearly were required to guide model calibrations in this study. Interpretations should improve with access to larger numbers of environmental tracers, longer time series of multiple tracers, inclusion of other chemical and isotopic data, improved subsurface geologic characterization, and enlightened spatial (visual) integration of these data. It is possible that a relatively detailed transport model calibrated with distributed data at one location could serve as a guide for lumped-parameter models at other nearby geologically similar sites.

Acknowledgements Groundwater-flow models with particle tracking described in this paper were constructed by K. Burow, B. Clark, C. Crandall, and J. Starn. This work was funded by the USGS National Water-Quality Assessment (NAWQA) Program and the USGS National Research Program. Manuscript reviews by C.T. Green, L.N. Plummer, C.S. Bayari, and several anonymous reviewers are greatly appreciated. The use of trade, product, or firm names in this report is for descriptive purposes only and does not imply endorsement by the US Government.

References

- Aeschbach-Hertig W, Peeters F, Beyerle U, Kipfer R (1999) Interpretation of dissolved atmospheric noble gases in natural waters. *Water Resour Res* 35:2779–2792
- Aeschbach-Hertig W, Peeters F, Beyerle U, Kipfer R (2000) Palaeotemperature reconstruction from noble gases in ground water taking into account equilibration with entrapped air. *Nat* 405:1040–1044
- Amin IE, Campana ME (1996) A general lumped parameter model for the interpretation of tracer data and transit time calculation in hydrologic systems. *J Hydrol* 179:1–21
- Bayer R, Schlosser P, Banisch G, Rupp H, Zaucker F, Zimmek G (1989) Performance and blank components of a mass spectrometric system for routine measurement of helium isotopes and tritium by the ^3He in-growth method. In: *Sitzungsberichte der Heidelberger Akademie der Wissenschaften, Mathematisch-naturwissenschaftliche Klasse*, 5. Springer, Heidelberg, Germany, pp 241–279
- Bethke CM, Johnson TM (2008) Groundwater age and groundwater age dating. *Annu Rev Earth Planet Sci* 36:121–152
- Böhlke JK (2002) Groundwater recharge and agricultural contamination. *Hydrogeol J* 10:153–179, Erratum: (2002) *Hydrogeol J* 10:438–439
- Böhlke JK (2006) TRACERMODEL1. Excel workbook for calculation and presentation of environmental tracer data for simple groundwater mixtures. In: *Use of chlorofluorocarbons in hydrology, a guidebook*, IAEA STI/PUB/1238. IAEA, Vienna, Austria, pp 239–243
- Brown CJ, Starn JJ, Stollenwerk KG, Mondazzi RA, Trombley TJ (2009) Aquifer chemistry and transport processes in the zone of contribution to a public-supply well in Woodbury, Connecticut, 2002–06. *US Geol Surv Sci Invest Rep 2009–5051*, 158 pp
- Burow KR, Jurgens BC, Kauffman LJ, Phillips SP, Dalgish BA, Shelton JL (2008) Simulations of groundwater flow and particle pathline analysis in the zone of contribution of a public-supply well in Modesto, eastern San Joaquin Valley, California. *US Geol Surv Sci Invest Rep 2008–5035*, 41 pp
- Busenberg E, Plummer LN (1992) Use of chlorofluoromethanes (CCl_3F and CCl_2F_2) as hydrologic tracers and age-dating tools, Example: the alluvium and terrace system of Central Oklahoma. *Water Resour Res* 28(9):2257–2283
- Busenberg E, Plummer LN, Bartholomay RC, and Wayland JE (1998) Chlorofluorocarbons, sulfur hexafluoride, and dissolved permanent gases in ground water from selected sites in and near the Idaho National Engineering and Environmental Laboratory, Idaho, 1994–97. *US Geol Surv Open-File Rep 98–274*, 72 pp
- Busenberg E, Plummer LN (2000) Dating young groundwater with sulfur hexafluoride, natural and anthropogenic sources of sulfur hexafluoride. *Water Resour Res* 36:3011–3030
- Busenberg E, Plummer LN (2006) Potential use of other atmospheric gases. In: *Use of chlorofluorocarbons in hydrology, a guidebook*, IAEA STI/PUB/1238. IAEA, Vienna, Austria, pp 183–190
- Carle SF (1999) T-PROGS: Transition probability geostatistical software: user's manual. University of California, Davis, CA
- Carle SF, LaBolle EM, Weissmann GS, VanBrocklin D, Fogg GF (1998) Geostatistical simulation of hydrostratigraphic architecture, a transition probability/Markov approach. In: *Fraser GS, Davis JM (eds) Concepts in hydrogeology and environmental geology no. 1: hydrogeologic models of sedimentary aquifers*. SEPM (Society for Sedimentary Geology), Tulsa, OK
- Chorco Alvarado JA, Purtschert R, Barbécot F, Chabault C, Ruedi J, Schneider V, Aeschbach-Hertig W, Kipfer R, Loosli HH (2007) Constraining the age distribution of highly mixed groundwater using ^{39}Ar , a multiple environmental tracer ($^3\text{H}/^3\text{He}$, ^{85}Kr , ^{39}Ar , and ^{14}C) study in the semiconfined Fontainebleau Sands Aquifer (France). *Water Resour Res*. doi:10.1029/2006WR005096
- Clark WB, Jenkins WJ, Top Z (1976) Determination of tritium by mass spectrometric measurement of ^3He . *Int J Appl Radiat Isot* 27:515–522
- Clark BR, Landon MK, Kauffman LJ, Hornberger GZ (2007) Simulations of groundwater flow, transport, age, and particle tracking near York, Nebraska, for a study of transport of anthropogenic and natural contaminants (TANC) to public-supply wells. *US Geol Surv Sci Invest Rep 2007–5068*, 48 pp
- Cook PG, Böhlke JK (2000) Determining timescales for groundwater flow and solute transport. In: *Cook PG, Herczeg AL (eds) Environmental tracers in subsurface hydrology*. Kluwer, Boston, pp 1–30
- Cook PG, Solomon DK (1995) Transport of atmospheric trace gases to the water table: Implications for groundwater dating with chlorofluorocarbons and krypton 85. *Water Resour Res* 31:263–270
- Crandall CA, Kauffman LJ, Katz BG, Metz PA, McBride WS, Berndt MP (2009) Simulations of groundwater flow and particle tracking analysis in the area contributing recharge to a public-supply well near Tampa, Florida, 2002–05. *US Geol Surv Sci Invest Rep 2008–5231*, 53 pp
- Eberts SM, Erwin ML, Hamilton PA (2005) Assessing the vulnerability of public-supply wells to contamination from urban, agricultural, and natural sources. *US Geol Surv Fact Sheet FS 2005–3022*, 4 pp
- Einarson MD, Mackay DM (2001) Predicting impacts of ground water contamination. *Environ Sci Technol* 35:66A–73A
- Frind EO, Molson JW, Rudolph DL (2006) Well vulnerability: a quantitative approach for source water protection. *Ground Water* 44:732–742
- Fylstra D, Lasdon L, Watson J, Waren A (1998) Design and use of the Microsoft Excel Solver. *Interfaces* 28:29–55
- Goode DJ (1996) Direct simulation of groundwater age. *Water Resour Res* 32:289–296
- Green CT, Böhlke JK, Bekins B, Phillips S (2010) Mixing effects on apparent reaction rates and isotope fractionation during denitrification in a heterogeneous aquifer. *Water Resour Res* 46:1–19
- Halford KJ, Hanson RT (2002) User guide for the drawdown-limited, multi-node well (MNW) package for the U.S. Geological Survey's modular three-dimensional finite-difference groundwater flow model, versions MODFLOW-96 and MODFLOW-2000. *US Geol Surv Open-File Rep 02–293*, 33 pp
- Harbaugh AW, Banta ER, Hill MC, McDonald MG (2000) MODFLOW-2000, the U.S. Geological Survey modular ground-water model: user guide to modularization concepts and the ground-water flow process. *US Geol Surv Open-File Rep 00–92*, 121 pp
- Heaton THE, Vogel JC (1981) Excess air in groundwater. *J Hydrol* 50:201–216
- Hill MC, Banta ER, Harbaugh AW, Anderman ER (2000) MODFLOW-2000, the U.S. Geological Survey modular ground-water model: user guide to the observation, sensitivity, and parameter-estimation processes and three post-processing programs. *US Geol Surv Open-File Rep 00–184*, 209 pp
- IAEA/WMO (2006) Global network of isotopes in precipitation, the GNIP Database. Available via <http://isohis.iaea.org>. Cited 27 Jan 2007
- Jurgens BC, Burow KR, Dalgish BA, Shelton JL (2008) Hydrogeology, water chemistry, and factors affecting the transport of contaminants in the zone of contribution of a public-supply well in Modesto, eastern San Joaquin Valley, California. *US Geol Surv Sci Invest Rep 2008–5156*, 78 pp

- Katz BG, Crandall CA, Metz PA, McBride WS, Berndt MP (2007) Chemical characteristics, water sources and pathways, and age distribution of ground water in the contributing recharge area of a public-supply well near Tampa, Florida, 2002–05. US Geol Surv Sci Invest Rep 2007–5139, 85 pp
- Kauffman LJ, Baehr, AL, Ayers, MA, Stackelberg, PE (2001) Effects of land use and travel time on the distribution of nitrate in the Kirkwood-Cohansey aquifer system in southern New Jersey. US Geol Surv Sci Invest Rep 01–4117, 49 pp
- Konikow LF, Hornberger GZ (2006) Use of the multi-node well (MNW) package when simulating solute transport with the MODFLOW ground-water transport process. US Geol Surv Tech Methods 6-A15, 34 pp
- Konikow LF, Goode DJ, Hornberger GZ (1996) A three-dimensional method-of- characteristics solute-transport model (MOC3D). US Geol Surv Water Resour Invest Rep 96–4267, 87 pp
- Koterba MT, Wilde FD, Lapham WW (1995) Ground-water data-collection protocols and procedures for the National Water-Quality Assessment Program: collection and documentation of water-quality samples and related data. US Geol Surv Open-File Rep 95–399, 113 pp
- Landon MK, Eberts SM, Jurgens BC, Katz BG, Burow KR, Crandall CA, Brown CJ, Starn JJ (2006) Knowledge of where and how contamination-susceptible water enters public-supply wells can be used to improve monitoring strategies and protection plans. Ground Water Protection Council Annual Forum. GWPC, Miami Beach, FL
- Landon MK, Clark BR, McMahon PB, McGuire VL, Turco MJ (2008) Hydrogeology, chemical-characteristics, and water sources and pathways in the zone of contribution of a public-supply well in York, Nebraska. US Geol Surv Water Resour Invest Rep 2008–5050, 149 pp
- Levenspiel O (1999) Chemical Reaction Engineering, 3rd edn. Wiley, New York
- Maloszewski P, Zuber A (1982) Determining the turnover time of groundwater systems with the aid of environmental tracers: 1, models and their applicability. J Hydrol 57:207–231
- Maloszewski P, Zuber A (1993) Principals and practice of calibration and validation of mathematical models for the interpretation of environmental tracer data in aquifers. Adv Water Res 16:173–190
- Maloszewski P, Zuber A (1996) Lumped parameter models for interpretation of environmental tracer data. Manual on mathematical models in isotope hydrogeology, IAEA-TECDOC-910. IAEA, Vienna, Austria, pp 9–58
- Manning AH, Solomon DK, Thiros SA (2005) $^3\text{H}/^3\text{He}$ age data in assessing the susceptibility of wells to contamination. Ground Water 43:353–367
- Maupin MA, Barber NL (2005) Estimated withdrawals from principal aquifers in the United States, 2000. US Geol Surv Circ 1279, 49 pp
- McMahon PB, Böhlke JK, Kauffman LJ, Kipp KL, Landon MK, Crandall CA, Burow KR, Brown CJ (2008a) Source and transport controls on the movement of nitrate to public supply wells in selected principal aquifers of the United States. Water Resour Res. doi:10.1029/2007WR006252
- McMahon PB, Burow KR, Kauffman LJ, Eberts SM, Böhlke JK, Gurdak JJ (2008b) Simulated response of water quality in public supply wells to land-use change. Water Resour Res. doi:10.1029/2007WR006731
- Michel RL (1989) Tritium deposition in the continental United States, 1953–83. US Geol Surv Water Resour Invest Rep 89–4072, 46 pp
- Michigan DEQ (2009) Use of tritium in assessing aquifer vulnerability. Michigan Department of Environmental Quality WHP 1–109. Available online. http://www.michigan.gov/documents/deq/deq-wb-dwehs-swpu-tritiumanalysisguidance_212715_7.pdf. Cited 10 Nov 2009
- Nelms DL, Harlow GE Jr, Plummer LN, Busenberg E (2003) Aquifer susceptibility in Virginia, 1998–2000. US Geol Surv Water Resour Invest Rep 03–4278, 58 pp
- Nir A (1986) Role of tracer methods in hydrology as a source of physical information: basic concepts and definitions—time relationship in dynamic systems. In: Mathematical models for interpretation of tracer data in groundwater hydrology, IAEA TECDOC-381. IAEA, Vienna, Austria, pp 7–44
- Osenbrück K, Fiedler S, Knöller K, Weise SM, Sültenfuß J, Oster H, Strauch G (2006) Timescales and development of ground-water pollution by nitrate in drinking water wells of the Jahna-Aue, Saxonia, Germany. Water Resour Res. doi:10.1029/2006WR004977
- Ozyurt NN, Bayari CS (2005) Steady- and unsteady-state lumped parameter modelling of tritium and chlorofluorocarbons transport: hypothetical analyses and application to an alpine karst aquifer. Hydrol Proc 19:3269–3284
- Paschke SS, Kauffman LJ, Eberts SM, Hinkle SR (2007) Overview of regional studies of the transport of anthropogenic and natural contaminants to public-supply wells. In: Hydrogeologic settings and ground-water flow simulations for regional studies of the transport of anthropogenic and natural contaminants to public-supply wells—studies begun in 2001. US Geol Surv Prof Pap 1737-A, 1-1-1-18
- Peeters F, Beyerle U, Aeschbach-Hertig W, Holocher J, Brennwald MS, Kipfer R (2002) Improving noble gas based paleoclimate reconstruction and groundwater dating using $^{20}\text{Ne}/^{22}\text{Ne}$ ratios. Geochim Cosmochim Acta 67:587–600
- Plummer LN, Busenberg E (2000) Chlorofluorocarbons, tools for dating and tracing young groundwater. In: Cook PG, Herczeg AL (eds) Environmental tracers in subsurface hydrology. Kluwer, Boston
- Plummer LN, Busenberg E (2006) Chlorofluorocarbons in the atmosphere. In: Use of chlorofluorocarbons in hydrology, a guidebook, IAEA STI/PUB/1238. IAEA, Vienna, Austria, pp 9–15
- Plummer LN, Busenberg E, Böhlke JK, Nelms DL, Michel RL, Schlosser P (2001) Groundwater residence times in Shenandoah National Park, Blue Ridge Mountains, Virginia, USA, a multi-tracer approach. Chem Geol 179:93–111
- Plummer LN, Busenberg E, Eberts SM, Bexfield LM, Brown CJ, Fahlquist LS, Katz BG, Landon MK (2008) Low-level detections of halogenated volatile organic compounds in groundwater, use in vulnerability assessments. J Hydrol Eng 13:1049–1068
- Poeter EP, Hill MC, Banta ER, Mehl S, Christensen S (2005) UCODE_2005 and six other computer codes for universal sensitivity analysis, calibration, and uncertainty evaluation. US Geol Surv Tech Methods 6-A11, 283 pp
- Pollock DW (1994) User's guide for MODPATH/MODPATH-PLOT, Version 3: a particle tracking post-processing package for MODFLOW, the U.S. Geological Survey finite-difference ground-water flow model. US Geol Surv Open File Rep 94–464, variously paginated
- Rupert MG, Plummer LN (2009) Groundwater quality, age, and probability of contamination, Eagle River Watershed valley-fill aquifer, North-Central Colorado, 2006–2007. US Geol Surv Water Resour Invest Rep 2009–5082, 59 pp
- Scanlon BR, Mace RE, Barrett ME, Smith B (2003) Can we simulate regional groundwater flow in a karst system using equivalent porous media models? Case study, Barton Springs Edwards aquifer, USA. J Hydrol 276:137–158
- Schlosser P, Stute M, Sonntag C, Munnich KO (1989) Tritogenic ^3He in shallow groundwater. Earth Planet Sci Lett 94:245–256
- Solomon DK, Cook PG (2000) ^3H and ^3He . In: Cook PG, Herczeg AL (eds) Environmental tracers in subsurface hydrology. Kluwer, Boston
- Solomon DK, Poreda RJ, Schiff SL, Cherry JA (1992) Tritium and Helium 3 as groundwater age tracers in the Borden Aquifer. Water Resour Res 28:741–755
- Spitz FJ (2001) Method and computer programs to improve pathline resolution near weak sinks representing wells in MODFLOW and MODPATH ground-water-flow simulations. US Geol Surv Open File Rep 00–392, 41 pp

- Starn JJ, Brown CJ (2007) Simulations of ground-water flow and residence time near Woodbury, Connecticut. US Geol Surv Sci Invest Rep 2007-5210, 45 pp
- Stewart JW, Goetz CL, Mills LR (1978) Hydrogeologic factors affecting the availability and quality of ground water in the Temple Terrace area, Hillsborough County, Florida. US Geol Surv Water Res Invest Rep 78-4, 38 pp
- Vogel JC (1967) Investigation of groundwater flow with radiocarbon. In: Isotopes in hydrology. IAEA, Vienna, Austria, pp 355-369
- Weissmann GS, Zhang Y, LaBolle EM, Fogg GE (2002) Dispersion of groundwater age in an alluvial aquifer system. *Water Resour Res* 38:1-8
- Zinn BA, Konikow LF (2007) Potential effects of regional pumpage on groundwater age distribution. *Water Resour Res.* doi:[10.1029/2006WR004865](https://doi.org/10.1029/2006WR004865)
- Zoellmann K, Kinzelbach W, Fulda C (2001) Environmental tracer transport (^3H and SF_6) in the saturated and unsaturated zones and its use in nitrate pollution management. *J Hydrol* 240:187-205
- Zuber A (1986) On the interpretation of tracer data in variable flow systems. *J Hydrol* 86:45-57
- Zuber A, Witeczak S, Róžański K, Śliwka I, Opoka M, Mochalski P, Kuc T, Karlikowska J, Kania J, Jackowicz-Korczyński M, Duliński M (2005) Groundwater dating with ^3H and SF_6 in relation to mixing patterns, transport modeling and hydrogeochemistry. *Hydrol Proc* 19:2247-2275